

Extensive Air Showers from Ultra High Energy Gluinos

V. Berezhinsky¹, M. Kachelrieß², and S. Ostapchenko^{3,4}

¹*INFN, Lab. Naz. del Gran Sasso, I-67010 Assergi (AQ)*

²*TH Division, CERN, CH-1211 Geneva 23*

³*Forschungszentrum Karlsruhe, Institut für Kernphysik, D-76021 Karlsruhe, Germany*

⁴*Moscow State University, Institute of Nuclear Physics, 199899 Moscow, Russia*

August 31, 2001

Abstract

We study the proposal that the cosmic ray primaries above the Greisen-Zatsepin-Kuzmin (GZK) cutoff are gluino-containing hadrons (\tilde{g} -hadrons). We describe the interaction of \tilde{g} -hadrons with nucleons in the framework of the Gribov-Regge approach using a modified version of the hadronic interaction model QGSJET for the generations of Extensive Air Showers (EAS). There are two mass windows marginally allowed for gluinos: $m_{\tilde{g}} \lesssim 3$ GeV and $25 \lesssim m_{\tilde{g}} \lesssim 35$ GeV. Gluino-containing hadrons corresponding to the second window produce EAS very different from the observed ones. Light \tilde{g} -hadrons corresponding to the first gluino window produce EAS similar to those initiated by protons, and only future detectors can marginally distinguish them. We propose a beam-dump accelerator experiment to search for \tilde{g} -hadrons in this mass window. We emphasize the importance of this experiment: it can discover (or exclude) the light gluino and its role as a cosmic ray primary at ultra high energies.

PACS numbers: 98.70.Sa, 14.80.-j

1 Introduction

Since long time light gluinos have attracted attention as a possible carrier of the very high energy signal in the universe. In the 80s, they were studied as a possible primary particle from Cyg X-3 [1, 2], now as a primary particle of the observed Ultra High Energy Cosmic Rays (UHECR) [3, 4].

The observations of UHECR with energies above 10^{20} eV impose a serious problem (see [5] for recent reviews).

The data show the presence of a new, nearly isotropic component in the UHECR flux above the energy $E \sim 10^{19}$ eV [5]. Since the arrival directions of the UHECR show no correlation with the galactic plane and the galactic magnetic field cannot isotropize particles of such energies, this component is thought to be extragalactic. On the other hand, the signature of extragalactic protons, the Greisen-Zatsepin-Kuzmin (GZK) cutoff [6] at $E \simeq 6 \cdot 10^{19}$ eV, is not found. The other natural UHE primaries, nuclei and photons, must also suffer a similar cutoff. Meanwhile, four different UHECR experiments [5] do not show the presence of such a cutoff. The two highest energy events are detected by AGASA [7] and Fly's Eye [8] at energy $2 \cdot 10^{20}$ eV and $3 \cdot 10^{20}$ eV, respectively. The total number of events with energy higher than $1 \cdot 10^{20}$ eV is about 30, 17 of which are detected by AGASA [9]. The accuracy of the energy determination is estimated to be better than 20–30%. The energies of the two highest energy events [7] and [8] are determined very reliably.

To resolve this puzzle, it seems that new ideas in astrophysics or particle physics are required.

The proposals involving particle physics include UHE particles from superheavy dark matter [10] and topological defects [11], the resonant interaction of UHE neutrinos with dark matter neutrinos [12], strongly interacting neutrinos [13], new particles as UHE primaries [3, 4, 14] and such a radical possibility as Lorentz invariance violation [15]. (For more references see also the reviews cited in [5].)

In this paper, we shall consider a gluino-containing hadron (\tilde{g} -hadron) as a carrier of the cosmic UHE signal, being inspired by the correlation between AGN and arrival directions of UHE particles suggested by the analyses in Refs. [4, 16]. This correlation implies that the signal carrier is neutral and is not absorbed by the CMBR. The light gluino is a suitable candidate for such a primary: it can be efficiently produced in pp-interactions in astrophysical sources, it is not strongly absorbed by CMBR (see below) and it produces EAS in the atmosphere very similar to those observed.

Heavy gluinos are naturally produced in decays of superheavy particles [17].

We shall study here the interaction of both light and heavy gluinos with nucleons at UHE. In most interesting applications gluinos must be light (see below). To be a suitable primary of UHECR, the \tilde{g} -hadron should satisfy three conditions:

1. The longitudinal shower profile of Fly's Eye highest energy event with $E = 3 \cdot 10^{20}$ eV is well fitted by a proton [18, 19], though Fly's Eye collaboration does not exclude a photon as a primary [8]. Therefore, \tilde{g} -hadrons should essentially mimic proton (or photon) induced air showers.

2. To shift the GZK cutoff to higher energies, the new hadron should have a mass in excess of the proton mass: the threshold energy for any energy-loss reaction on microwave photons increases with increasing primary mass, while the fraction of energy lost per scattering decreases. Moreover, it is desirable that its cross-section for interactions with CMBR photons is smaller than the proton's one. This can be achieved if, e.g., the mass of the first resonance X that can be excited in the reaction \tilde{g} -hadron + $\gamma_{\text{CMBR}} \rightarrow X$ is relatively large.
3. The primary has to be stable or quasi-stable with lifetime $\tau \gtrsim 10^6 \text{s} (m/\text{GeV})(L/\text{Gpc})$ in order to survive its travel from a source (e.g. AGN) at distance $L \sim 100\text{--}1000$ Mpc to the Earth.

In principle gluino-containing hadrons (\tilde{g} -hadrons) could satisfy the above requirements. Below we shall shortly review the status of \tilde{g} -hadrons as UHECR signal carrier.

To satisfy the third condition, the gluino should be the Lightest Supersymmetric Particle (LSP), or have a very small mass difference with the LSP. It also can be the second lightest supersymmetric particle, if the LSP is the gravitino; in this case the gluino decays gravitationally and its lifetime can be long enough. Theoretically the best motivated candidates for the LSP are the neutralino and gravitino. While in minimal supergravity models the LSP is the lightest neutralino (in some part of the parameter space it is the sneutrino), in models with gauge-mediated SUSY the LSP is normally the gravitino. In Farrar's model [20], the gluino is the LSP because the dimension-three SUSY breaking terms are set to zero. A theoretically more appealing scenario containing a light gluino was developed in Refs. [21, 22]. There, the gluino with mass 1–100 GeV was found in a SO(10) model with gauge-mediated SUSY breaking and Higgs-messenger mixing. In this model either the gluino or the gravitino is the LSP. In the latter case, the gluino can decay but has a sufficiently long lifetime to be a viable UHECR primary, $\tau \sim 100$ yr.

In a physical state, the gluino is bound into colourless hadrons. What is the lightest state of gluino-containing hadrons?

In the 80s (see [2]), it was argued on the basis of QCD sum rules that the *glueballino* $\tilde{g}g$ is the lightest \tilde{g} -hadron. The lightest baryonic state, *gluebarino*, was demonstrated to be the $\tilde{g}uud$ -hadron [23]. Gluebarino is a long-lived particle because its decay needs either violation of baryon number or R-parity [23]. More recently, Farrar proposed [20] the neutral hadron S^0 , a $\tilde{g}uds$ bound-state, as the lightest \tilde{g} -hadron (see also the calculations in the MIT bag model of Ref. [24]).

There is some controversy if a light gluino, with a mass of a few GeV, is allowed. As it stands, the Farrar model [20] is in conflict with searches for glueballino decays [25, 26, 27] as well as for decays of other unstable \tilde{g} -hadrons [28]. However, these searches had been restricted to a narrow band of lifetimes and masses, and their results are not valid in the context of more generic models.

The existence of a light gluino ($m_{\tilde{g}} \lesssim 5$ GeV) can be (dis-) proved due to its contribution to the running of α_s and to QCD colour coefficients in a practically model-independent way. The authors of Ref. [29] used the ratio R between the hadronic and the $\bar{\mu}\mu$ production cross-section in e^+e^- annihilation at different energies to constrain the light gluino scenario. They excluded light gluinos with mass $m_{\tilde{g}} = 3(5)$ GeV with 93(91)% CL, while

the mass range ≤ 1.5 GeV remained essentially unconstrained. Combining these results with the determination of QCD colour coefficients from the analysis of multi-jet events in [30], the conclusions of [29] became much stronger: light gluinos with mass ≤ 5 GeV were excluded with at least 99.89% CL. The analysis of multi-jet events relied however on the use of Monte Carlo simulations which parameters are tuned to QCD without light gluinos. Moreover, the multi-jet analysis was based on a tree-level calculation with rather large scale ambiguities. The assessment of these uncertainties is difficult, thus preventing the definite exclusion of a very light gluino by this argument [31, 32].

Direct accelerator limits for the gluino as LSP were discussed recently in Refs. [22, 33, 34]: The authors of Ref. [33] concluded that the range $3 \text{ GeV} \lesssim m_{\tilde{g}} \lesssim 130\text{--}150 \text{ GeV}$ can be excluded at 95% C.L. based on currently available OPAL and CDF data. Their results are sensitive to the details of the hadronic interactions of \tilde{g} -hadrons and, for certain choices of the parameters, a window in the intermediate mass region $23 \text{ GeV} \lesssim m_{\tilde{g}} \lesssim 50 \text{ GeV}$ remains open. Meanwhile, Ref. [22] noted that these limits could be weakened if squarks are not very heavy and contribute to the jet + missing energy signal, while Ref. [34] confirmed an open window for a gluino with $25 \text{ GeV} \lesssim m_{\tilde{g}} \lesssim 35 \text{ GeV}$.

We also mention here that cosmological constraints do not exclude both light and heavy gluinos of interest [17, 35].

The Gustafson experiment [37] does not exclude \tilde{g} -hadrons (see section 5).

Till now we discussed the limits on the gluino mass $m_{\tilde{g}}$. The lightest \tilde{g} -hadron with mass $M_{\tilde{g}}$ is heavier than the gluino by the mass of its constituent gluon or quarks, which are expected to be less than 1 GeV.

Light \tilde{g} -hadrons with $M_{\tilde{g}} \sim 1.5$ GeV have a spectrum with the GZK cutoff beyond the currently observed energy range (see [17] and Fig. 12 of the present paper). Together with the accelerator limits on gluino masses this leaves a narrow band of allowed masses for the light \tilde{g} -hadrons at $1.5 \lesssim M_{\tilde{g}} \lesssim 4$ GeV. But this window is closed if, as argued in [23], the charged gluebarino $\tilde{g}uud$ is lighter than the neutral $\tilde{g}uds$. Indeed, production of charged gluebarinos in the Earth atmosphere by cosmic rays and their accumulation in the ocean results in too high abundance of “wild hydrogen” in contradiction with observational data. In Refs. [20, 24], however, it is argued that the lightest gluebarino is the neutral flavour singlet $\tilde{g}uds$, due to strong quark attraction in this state. But even in this case the restriction [23] might work, if $\tilde{g}uds$ -gluebarino and proton are bound into anomalous deuterium.

In conclusion, a light gluino—although being disfavoured by various arguments—is not excluded. We are studying here the interactions of gluinos, being inspired by a possible correlation between AGN and the arrival directions of UHECR [4, 16] and by the recent suggestion [3, 38], that Extensive Air Showers (EAS) observed at the highest energies could be produced by \tilde{g} -hadrons. The authors of Ref. [38] performed a detailed simulation of EAS induced by \tilde{g} -hadrons, using however a phenomenological description for the \tilde{g} -hadron-nucleon interaction which is not self-consistent. They found that masses as high as 50 GeV are compatible with presently available data. In contrast, it was argued in Ref. [17], using kinematical arguments, that the observed shower characteristics exclude any strongly interacting particle much heavier than a few GeV.

The purpose of the present work is to study EAS produced by \tilde{g} -hadrons and to restrict

the mass range in which the \tilde{g} -hadron is a viable UHE primary using a self-consistent interaction model. We have used for the simulation of air showers initiated by \tilde{g} -hadrons a suitably modified version of the QGSJET model [39, 40] which is known to describe successfully proton air showers [39, 41]. Specifically, we have considered the glueballino as the \tilde{g} -hadron but we expect that our results apply to all \tilde{g} -hadrons. We paid special attention to consistent calculations of glueballino-hadron interaction cross-sections and of cascade particle production in the atmosphere. We have found that the development of showers initiated by \tilde{g} -hadrons with masses above 5 GeV differs substantially from proton-initiated showers and is inconsistent with the current experimental data. In the window of masses 1.5–4 GeV, where a \tilde{g} -hadron can be allowed, glueballino-induced showers do not contradict the available data. Future observations by the detectors HiRes and Auger can either confirm or exclude \tilde{g} -hadrons as the dominant primary combining the information from shower profiles and energy spectrum. However, the best way to test this hypothesis is a modified Gustafson experiment (see Section 5). In the case of the discovery of light \tilde{g} -hadrons in such an experiment we shall reliably know their properties, thus enabling us to calculate the production of these particles in astrophysical sources and their detection in the Earth atmosphere. Their absence will preclude further discussion of this hypothesis.

2 Glueballino–proton (nucleus) interaction

2.1 QGSJET framework

QGSJET, a Monte Carlo generator of hadron-hadron, hadron-nucleus, and nucleus-nucleus interactions [39, 40], was developed in the framework of the Gribov-Regge approach and is based on the quark-gluon string model of the supercritical Pomeron [42]. Hadronic interactions are described as a superposition of elementary rescattering processes between the partonic constituents of the projectile and target nucleons (hadrons), resulting in the production of colour neutral strings, which further fragment into secondary hadrons. The key parameters of the model are the intercepts and the slopes of the Regge trajectories of the Pomeron and of secondary Reggeons. These parameters govern the formation of different interaction configurations, how the energy-momentum is shared in elementary interactions, and also the string hadronization. The model was generalized to hadron-nucleus and nucleus-nucleus interactions in the framework of the Glauber-Gribov approach [43, 44], taking into account low mass diffraction and inelastic screening processes [45]. Hard QCD processes were included into the Gribov-Regge formalism via the concept of a "semihard Pomeron", which is a t -channel iteration of the soft Pomeron and a QCD parton ladder contribution [40, 46].

QGSJET describes hadron-hadron interaction amplitudes as a sum of two contributions, namely soft and semihard rescatterings [40]. The soft contributions are of purely nonperturbative nature and correspond to the case of a parton cascade with virtualities smaller than some cutoff Q_0^2 . Below this cutoff, perturbative QCD is not applicable and the interaction is described by phenomenological soft Pomeron exchange. The amplitude

$f_{ac}^{\mathbb{P}}$ for Pomeron exchange between two hadrons a and c is given by [42]

$$f_{ac}^{\mathbb{P}}(s, b) = \frac{\gamma_a \gamma_c \exp(\Delta y)}{\lambda_{ac}(y)} \exp\left(-\frac{b^2}{4\lambda_{ac}(y)}\right) \quad (1)$$

$$\lambda_{ac}(y) = R_a^2 + R_c^2 + \alpha'_{\mathbb{P}} y, \quad (2)$$

where $y = \ln s$ is the rapidity size of the Pomeron, s is the squared center-of-mass energy for the interaction, b is the impact parameter between the two hadrons, and the parameters $\gamma_{a(c)}$, $R_{a(c)}^2$ are the vertices and slopes for the Pomeron-hadron $a(c)$ coupling, respectively. Finally, Δ and $\alpha'_{\mathbb{P}}$ are the parameters describing the overcriticality and the slope of the soft Pomeron trajectory.

Contrary to soft rescatterings, semi-hard ones correspond to the case when at least a part of the parton cascade develops in the region of parton virtualities $q^2 > Q_0^2$ and, therefore, can be described on the basis of QCD techniques. The complete semi-hard contribution is represented by a QCD parton ladder sandwiched between two soft Pomerons [46]. For the Pomeron, the formulas (1-2) can still be used. However, since it is now coupled to a hadron $a(c)$ on one side but to a parton ladder on the other side, the slope $R_{c(a)}^2$ and the coupling $\gamma_{c(a)}$ have to be replaced by the slope R_{lad}^2 and the coupling $V_{\text{lad}}^{\mathbb{P}}$ of the Pomeron-ladder. The latter is parameterised as

$$V_{\text{lad}}^{\mathbb{P}}(y) = r [1 - \exp(-y)]^{\beta_{\mathbb{P}}}, \quad (3)$$

where the parameters r and $\beta_{\mathbb{P}}$ describe the momentum distribution of a parton (sea quark or gluon) in the soft Pomeron. Using $R_{\text{lad}}^2 \simeq 1/Q_0^2 \ll R_{a(b)}^2 + \alpha'_{\mathbb{P}} y$, the slope R_{lad}^2 can be neglected.

To complete the description of soft and semihard contributions, the momentum distribution function $N_a^{\mathbb{P}}$ for soft Pomeron emission by a hadron of type a has to be specified. It is parameterised in the form

$$N_a^{\mathbb{P}}(x_{\mathbb{P}}^{\pm}) \sim (x_{\mathbb{P}}^{\pm})^{\alpha} (1 - x_{\mathbb{P}}^{\pm})^{\beta_a}, \quad (4)$$

where the first factor does not depend on the hadron type and describes the probability to slow down the hadron constituents to which the Pomeron is connected. In QGSJET, the Pomeron is connected to a (dressed) quark-antiquark pair. Using Regge asymptotics [42], i.e. $\alpha_{q\bar{q}} \simeq 0.5$ as the intercept of the Regge $q\bar{q}$ -trajectory for light quarks, it follows

$$\alpha = 1 - 2\alpha_{q\bar{q}} \simeq 0. \quad (5)$$

Similar, the second factor in Eq. (4) describes the probability to slow down the "leading" hadron state configuration; the parameter β_a is expressed via the intercept $\alpha_{a\bar{a}}$ of the corresponding Regge trajectory as $\beta_a = -\alpha_{a\bar{a}}$.

The semihard contribution described above corresponds to the case that gluons or sea quarks of the hadron start the interaction at the initial scale Q_0^2 . Additionally, valence quarks can interact with $q^2 \geq Q_0^2$. Then the only nonperturbative input needed are the valence quark momentum distributions $q_v(x, Q_0^2)$ at the initial scale Q_0^2 .

2.2 Extension for glueballino

The nucleon-glueballino interaction can be treated in the QGSJET model in the same framework as the one for usual hadrons [39]. The main difficulty is to connect the unknown physical parameters (coupling $\gamma_{\tilde{G}}$, slope $R_{\tilde{G}}^2$ and momentum distribution $N_{\tilde{G}}^{\text{P}}$) describing the interactions of glueballinos with the corresponding quantities of usual hadrons. We use simple scaling arguments to derive the glueballino parameters from those of the pion:

1. The coupling γ_a of a hadron a to the Pomeron depends essentially on its size and, consequently, on its reduced mass M_a . If r_a denotes the radius of the hadron a with the reduced mass M_a , then $\gamma_a \sim r_a^2 \sim M_a^{-2}$, where we have neglected a factor $\alpha_s(M_a^2)$ in the last step. Thus, the Pomeron-glueballino vertex $\gamma_{\tilde{G}}$ can be expressed via the Pomeron-pion vertex γ_{π} as

$$\gamma_{\tilde{G}} = \gamma_{\pi} \left(\frac{M_{\pi}}{M_{\tilde{G}}} \right)^2. \quad (6)$$

For the reduced mass $M_{\tilde{G}}$ of the glueballino, we use

$$M_{\tilde{G}} = \frac{m_{\tilde{g}}m_g}{m_{\tilde{g}} + m_g}, \quad (7)$$

where $m_{\tilde{g}}$ is the mass of the gluino and $m_g \simeq 0.7$ GeV is the constituent mass of the gluon. Similar, we use for the pion $M_{\pi} = m_q/2$ with $m_q \simeq 0.35$ GeV as quark constituent mass. Note that Eq. (6) does not take into account the different colour factors of quarks and gluon/gluinos because we consider an effective Pomeron coupling to the hadron as a whole, not to individual parton constituents.

2. The slope $R_{\tilde{G}}^2$ for the Pomeron-glueballino coupling is also inverse proportional to $M_{\tilde{G}}^2$. Therefore, $R_{\tilde{G}}^2$ is small compared to R_p^2 and $R_{\text{P}}^2 = \alpha'_{\text{P}}y$ and can be neglected in the formulas (1-2),

$$\lambda_{\tilde{G}p}(y) \simeq R_p^2 + \alpha'_{\text{P}}y. \quad (8)$$

3. The momentum distribution for Pomeron emission is again given by Eq. (4), $N_{\tilde{G}}^{\text{P}} \sim (x_{\text{P}}^{\pm})^{\alpha}(1 - x_{\text{P}}^{\pm})^{\beta_{\tilde{G}}}$. Now the "leading" configuration consists of a valence gluon and gluino,

$$\beta_{\tilde{G}} = 1 + \beta_{\tilde{g}} + \beta_g. \quad (9)$$

Assuming that a valence gluon behaves similar to a valence $q\bar{q}$ -pair in the low x -limit gives $\beta_g \simeq 1 - 2\alpha_{q\bar{q}} \simeq 0$. The remaining unknown parameter $\beta_{\tilde{g}}$ can be found from the momentum distribution between the valence constituents of the glueballino. Using as ansatz for the momentum distribution $\rho_{\tilde{g}}^{\tilde{G}}$ of the gluino

$$\rho_{\tilde{g}}^{\tilde{G}}(x_{\tilde{g}}) \sim x_{\tilde{g}}^{\beta_{\tilde{g}}}(1 - x_{\tilde{g}})^{\beta_g} \quad (10)$$

and assuming that the energy is shared according to the constituent masses of the valence partons, we obtain for the average momentum fraction carried by the gluino

$$\langle x_{\tilde{g}} \rangle = \frac{m_{\tilde{g}}}{m_g + m_{\tilde{g}}} = \frac{\beta_{\tilde{g}} + 1}{\beta_g + \beta_{\tilde{g}} + 2}. \quad (11)$$

This results in

$$\beta_{\tilde{g}} = \frac{m_{\tilde{g}}}{m_g} (\beta_g + 1) - 1 \simeq \frac{m_{\tilde{g}}}{m_g} - 1. \quad (12)$$

Having fixed the free parameters describing the Pomeron-glueballino interactions using essentially only one simple, physically well-motivated scaling argument, the soft and semi-hard contributions are determined. These two contributions to the total nucleon-glueballino interaction are referred below as the contribution due to the *soft coupling*, because they are both caused by soft Pomeron emission of the glueballino.

To complete the formalism, we need to define the momentum distributions of the valence gluon or gluino inside the glueballino probed at the initial scale Q_0^2 , when they are involved into hard interactions. We shall refer to this contribution below as the contribution due to the *direct coupling*. Parton emission by a gluino in the s -channel is strongly suppressed kinematically in the nonperturbative region $q^2 < Q_0^2$ by its mass: the virtuality q^2 of the process $\tilde{g} \rightarrow g + \tilde{g}$ is determined by the off-shellness $|q_{\tilde{g}}^2 - M_{\tilde{g}}^2|$ of the produced t -channel gluino,

$$q_{\tilde{g} \rightarrow \tilde{g}}^2 = |q_{\tilde{g}}^2 - M_{\tilde{g}}^2| = \frac{p_{\perp}^2}{1-z} + M_{\tilde{g}}^2(1-z). \quad (13)$$

Here p_{\perp} and z are the transverse momentum and the light cone momentum fraction for the t -channel gluino. Therefore, the gluino momentum distribution at the scale Q_0^2 essentially remains in the form (10),

$$\tilde{g}_v(x_{\tilde{g}}, Q_0^2) = \rho_{\tilde{g}}^{\tilde{G}}(x_{\tilde{g}}). \quad (14)$$

By contrast, the momentum distribution of the valence gluon differs from $\rho_g^{\tilde{G}}(1-x_g)$ in (10) because of the emission of sea quarks and gluons (due to the soft coupling defined above),

$$g_v(x_g, Q_0^2) \sim x_g^{\beta_g} (1-x_g)^{\beta_{\tilde{g}}+\delta}. \quad (15)$$

The parameter δ is fixed by the momentum conservation constraint for the complete (valence and sea) parton momentum distributions at the initial scale Q_0^2 . This completes the formulation of the initial conditions for the perturbative evolution.

The treatment of the perturbative part of the interaction is performed to leading-log accuracy, the corresponding techniques are described in Ref. [39]. All emitted (s -channel) partons undergo timelike cascading according to the standard algorithm [47], with soft gluon coherence taken into account. At the final stage, soft strings are assumed to be formed between on-shell partons according to their colour connection pattern. The final gluino is assumed to pick up a gluon-gluon singlet pair from the vacuum. After a colour rearrangement similar to the one in J/ψ production, a glueballino is formed. String hadronization completes the procedure for glueballino-hadron interaction. The extension of the model to glueballino-nucleus collisions is based on the standard Glauber-Gribov approach and does not differ from the usual hadron-nucleus case [45].

2.3 Numerical results

The model developed in the last subsection allows both to calculate the cross-sections for glueballino-nucleon interactions and to treat consistently particle production in these reactions. Some quantities characterising the glueballino-nucleon interactions are given in Table 1 for $E_{\text{lab}} = 100$ GeV and in Table 2 for $E_{\text{lab}} = 10^{12}$ GeV. We present both total and inelastic cross-sections as well as the partial contributions arising due to the soft ($\sigma_{\text{tot}}^{\text{s-coupl.}}$) and direct ($\sigma_{\text{tot}}^{\text{d-coupl.}}$) coupling of the glueballino¹. At low energies, the soft coupling strongly dominates the \tilde{G} -proton interaction for all $M_{\tilde{G}}$ being governed by nonperturbative soft interactions, while the direct coupling can be neglected. At high energies, this picture changes considerably. The soft coupling becomes more and more suppressed for large $M_{\tilde{G}}$. By contrast, the direct contribution, which is purely perturbative on the glueballino side, is nearly independent of $M_{\tilde{G}}$. This important difference from the usual hadron case is due to the very asymmetric energy partition between parton constituents of the glueballino. For large $M_{\tilde{G}}$, the valence gluino carries almost the whole initial energy of the particle (88% for $M_{\tilde{g}} = 5$ GeV and 99% for $M_{\tilde{g}} = 50$ GeV) – Eqs. (10-11), (14), thus leaving just a small part of it to other partons, to which Pomerons are connected. Therefore, the glueballino behaves in the limit of large $M_{\tilde{G}}$ essentially as a perturbative object, as one expects from kinematical considerations [17]. Finally, the last row of the tables shows the inelasticity coefficient K_{inel} as another important quantity which distinguishes proton-proton and \tilde{G} -proton interactions. Although at energies of interest for UHECR the total cross-section for \tilde{G} -proton interactions is rather large, a heavy glueballino behaves like a penetrating particle in the atmosphere losing only a small part of its energy in one interaction. This conclusion was already reached in Ref. [17] from semiquantitative considerations. The reason for this effect is twofold. On one side, as discussed above, gluinos of larger masses carry a larger fraction of the initial particle energy, leaving a smaller part of it for the sea constituents ((anti-)quarks and gluons) and thus reducing the average number of multiple interactions in \tilde{G} -proton (nucleus) collisions. On the other hand, the relative weight of the "direct hard" process increases for heavier gluinos, where the valence gluino loses typically only a small part of its energy, as a large longitudinal momentum transfer is strongly suppressed in that case by the process virtuality $q_{\tilde{g} \rightarrow g}^2$,

$$q_{\tilde{g} \rightarrow g}^2 = \frac{p_{\perp}^2}{1-z} + \frac{z^2 M_{\tilde{g}}^2}{1-z}, \quad (16)$$

with p_{\perp} and z being the transverse momentum and the light cone momentum fraction for the t -channel gluon emitted of the initial valence gluino which mediates the gluino hard interaction with the target proton (nucleus).

We show also in Figs. 1 and 2 the total and inelastic cross-sections as function of the interaction energy E_{lab} for glueballino masses $M_{\tilde{G}} = 2, 5$ and 50 GeV. The fast increase of the direct contribution with E_{lab} produces an interesting effect: the total interaction cross-section for the largest glueballino mass considered, $M_{\tilde{G}} = 50$ GeV, which is dominated by

¹Note that the total cross section is smaller than the sum of the partial contributions $\sigma_{\text{tot}}^{\text{s-coupl.}}$ and $\sigma_{\text{tot}}^{\text{d-coupl.}}$, because it contains contributions from multiple rescatterings of both types.

the direct contribution, overshoots the ones for smaller glueballino masses in the energy range $10^4 - 10^9$ GeV.

3 Extensive air showers (EAS)

In this section, we present some results of our simulations for the glueballino-initiated EAS. Shower profiles and distributions of shower maxima are shown in Figs. 3–8 for three different initial energies, $E_0 = 10^{17}$, 10^{19} and 10^{20} eV, for the glueballino as primary with different choices of the gluino mass. For comparison, the case of a primary proton is also shown. At the highest energy considered, $E_0 = 10^{20}$ eV, the longitudinal shower profiles (Fig. 3) and the distribution of the shower maxima X_{\max} (Fig. 4) of glueballino-induced EAS are comparable with those induced by protons in the case of glueballino masses smaller than 5 GeV. As the glueballino mass increases, the shower develops deeper in the atmosphere with a less pronounced maximum. The fluctuations in X_{\max} increase also for larger glueballino masses. The main reason for both effects is the competition between the large glueballino-nucleus cross-section and the small inelasticity of the interactions: a heavy glueballino injects in one interaction only a small part of its energy into secondary hadronic and electromagnetic cascades, while interactions with a large momentum transfer are rare and increase only the fluctuations. Figure 4 clearly shows that the glueballino-induced EAS drastically differ from the proton-induced showers for glueballino masses larger than 5 GeV, and hence these showers can be distinguished even in case of low statistics. In case of a lighter glueballino with $M_{\tilde{G}} = 2$ GeV, a larger statistics is necessary to distinguish glueballino from proton, when only X_{\max} measurements are used. The same conclusions can be drawn comparing the shape of the calculated profiles for individual p - and \tilde{G} -induced EAS of energy $E_0 = 3.2 \cdot 10^{20}$ eV with the corresponding measurements of the Fly’s Eye collaboration [48], cf. Fig. 9. In doing so we choose only those showers which reach their maxima near the measured value $X_{\max} = 815 \pm 50$ g/cm². Then we average the obtained profiles and shift them to the same position of the shower maximum, $X_{\max} = 815$ g/cm². It is easy to see that for gluino masses larger than 5 GeV the shape of the calculated profile strongly disagrees with the experimental observations. The account for the LPM effect results in only 5% reduction of the electron number in the shower maximum for proton-induced EAS [19] and has an even smaller influence on the \tilde{G} -induced showers due to much softer π^0 -spectrum in the glueballino interactions.

The calculated lateral distribution functions (LDFs) for electrons and muons ($E_\mu > 1$ GeV) at the AKENO observation level (900 g/cm²) are shown in Figs. 10 and 11 for the proton and glueballinos with masses 2 and 5 GeV. The plotted values are the LDFs of electrons and muons $\rho_e(R)$, $\rho_\mu(R)$ at different distances R from the shower core. Although these distributions are substantially different for showers initiated by glueballinos and protons, they hardly can be used to search for the light glueballino on the basis of existing data, e.g., of AGASA. An adequate tool for the glueballino search is the fluctuation of the muon density at distances $R \gtrsim 300$ m from the core. This method allows in principle to discriminate showers initiated even by light glueballinos with $M_{\tilde{G}} \approx 2$ GeV from proton-initiated EAS (see Table 4).

Finally, we shall compare our results with those of Albuquerque, Farrar and Kolb (AFK) [38]. AFK have modified the event generator SIBYLL including the \tilde{g} -hadron (\tilde{G}) as a new particle. The interaction properties of \tilde{g} -hadron were taken *ad hoc*. Two assumptions were used for the total cross-section: $\sigma_{\text{tot}}(\tilde{G}p) \approx \sigma_{\text{tot}}(\pi p)$ (the favourite choice) and $\sigma_{\text{tot}}(\tilde{G}p) \approx 0.1\sigma_{\text{tot}}(\pi p)$. The mean energy fraction transferred from the \tilde{g} -hadron to the shower per interaction was modeled by a Peterson fragmentation function. Hard interactions with the production of minijets by the incident \tilde{g} -hadron were neglected.

It is easy to see that these modifications are not self-consistent. Indeed, on one hand the authors assume a large $\tilde{G}p$ cross-section, while on the other hand they neglect the hard processes (production of minijets), which give the dominant contribution to the $\tilde{G}p$ cross-section and make it large. In fact, our calculations explicitly show that at ultra-high energies the $\tilde{G}p$ cross-section and particle production are dominated by hard interactions for both light and heavy gluinos. For light gluinos, valence gluon and sea partons have enough momenta for hard interactions. For heavy gluinos, its own ("direct") hard interaction dominates. Soft interactions without the production of parton jets are negligible in both cases.

To elucidate the reason for the failure of the AFK approach, we have calculated the total \tilde{G} -nucleon cross-section switching off the hard interaction (cf. 5th entry, σ_{AFK} , in Table 1 and 2): At energies relevant for UHECR, the interactions considered by AFK are only subdominant and result in much smaller total cross-sections as compared with ours or those assumed by AFK.

4 Energy losses of glueballinos on CMBR photons and glueballino energy spectrum

Although both valence constituents of the glueballino are electrically neutral, UHE glueballinos lose energy due to scattering on CMBR photons. The value of the cutoff in its energy spectrum is determined by the transition from adiabatic energy losses (redshift) to rapidly increasing energy losses due to the reaction $\tilde{G} + \gamma \rightarrow \tilde{G} + \pi^0$ at higher energies. This process cannot occur due to π^0 exchange in the t -channel. The dominant contribution is given by the resonant formation of $\tilde{g}\bar{q}q$ states in the s -channel. The mass spectrum of $\tilde{g}\bar{q}q$ states was calculated as function of the gluino mass in Ref. [49] in the MIT bag model. The lowest $\tilde{g}\bar{q}q$ state found was the spin-1/2 state $\tilde{\rho}_{1/2}$; its mass difference to the glueballino is however, except for $m_{\tilde{G}} < 1.2$ GeV, too small as to allow the decay $\tilde{\rho}_{1/2} \rightarrow \tilde{G} + \pi^0$, cf. Table 6. We assume therefore that the first resonance in the s -channel is an excited $\tilde{\rho}_{1/2}^*$ state; for its mass $m(\tilde{\rho}_{1/2}^*)$ we use $m(\tilde{\rho}_{1/2}^*) = m(\tilde{\rho}_{1/2}) + 730$ MeV guided by the mass difference between the $\rho(770)$ and the $\rho(1400)$. The Breit-Wigner cross-section for the reaction $\tilde{G} + \gamma \rightarrow \tilde{\rho}_{1/2} \rightarrow \tilde{G} + \pi^0$ is [32]

$$\sigma(s) = \frac{2\pi}{p_{\text{cm}}^2} \frac{B_{\text{in}}B_{\text{out}}\Gamma_{\text{tot}}^2 m_{\tilde{\rho}}^2}{(s - m_{\tilde{\rho}}^2)^2 + (m_{\tilde{\rho}}\Gamma_{\text{tot}})^2}, \quad (17)$$

where p_{cm} and \sqrt{s} are the momentum and the total energy of the particles in the cm system, $m_{\tilde{\rho}}$ is the mass of the $\tilde{\rho}_{1/2}/\tilde{\rho}_{1/2}^*$ particle and Γ_{tot} is its total decay width. Finally,

B_{in} and B_{out} denote the branching ratios of the resonance to the initial and final states.

For the determination of the unknown branching ratios B_{in} , B_{out} and the total decay rate Γ_{tot} , we can use the analogy between the glueballino and the pion together with scaling arguments as in Sec. 2.2 both for the $\tilde{\rho}_{1/2}$ and the $\tilde{\rho}_{1/2}^*$. Then

$$B_{\text{out}} = \Gamma(\tilde{\rho}_{1/2} \rightarrow \tilde{G} + \pi^0) / \Gamma_{\text{tot}}(\tilde{\rho}_{1/2}) \simeq 1 \quad (18)$$

and

$$B_{\text{in}} = \frac{\Gamma(\tilde{\rho}_{1/2} \rightarrow \tilde{G} + \gamma)}{\Gamma_{\text{tot}}(\tilde{\rho}_{1/2})} \simeq \frac{\Gamma(\rho^0 \rightarrow \pi^0 + \gamma)}{\Gamma_{\text{tot}}(\rho)} \simeq 7 \cdot 10^{-4}. \quad (19)$$

The total decay rate $\Gamma_{\text{tot}}(\tilde{\rho}_{1/2}) \propto g_{\tilde{\rho}}^2 m_{\tilde{\rho}}$ can be calculated using $m_{\tilde{\rho}}$ from Ref. [49] together with

$$g_{\tilde{\rho}} = \frac{m_{\rho}}{m_{\tilde{\rho}}} g_{\rho}. \quad (20)$$

The maximum of the photo-pion production cross-section for the glueballino is at least a factor 8 smaller than for the proton due to the differences in B_{in} , the spin factors and p_{cm} . We neglect multipion production $\tilde{G} + \gamma \rightarrow \tilde{G} + \pi^+ + \pi^-$, which operates at energies above those we are interested in. The non-resonant contributions have been calculated in the vector dominance model and give only a small contribution to the total cross-section of the glueballino. The hard processes with gluon exchange are important only at high energies.

The energy loss of a particle scattering on CMBR photons is given by [50]

$$-\frac{1}{E} \frac{dE}{dt} = \frac{T}{2\pi^2 \Gamma^2} \int_{E_{\text{th}}}^{\infty} dE_r \sigma(E_r) y(E_r) E_r \left\{ -\ln \left[1 - \exp \left(-\frac{E_r}{2\Gamma T} \right) \right] \right\}. \quad (21)$$

Here, Γ is the Lorentz factor of the particle in the CMBR frame, E_r is the energy of a CMBR photon in the rest system of the glueballino, $E_{\text{th}} = m_{\pi}(1 + m_{\pi}/2m_{\tilde{G}})$ is the threshold energy in the glueballino rest system and y is the average fraction of energy lost by the glueballino in a collision, which for one-pion production is

$$y(E_r) = \frac{E_r}{m_{\tilde{G}}} \frac{1 + m_{\pi}^2/2E_r m_{\tilde{G}}}{1 + 2E_r/m_{\tilde{G}}}. \quad (22)$$

The energy spectrum dN/dE of glueballinos emitted by diffuse sources is at the present redshift $z = 0$ given by

$$\frac{dN}{dE}(0) = a \int_0^{z_{\text{max}}} dz_g (1 + z_g)^{-5/2} \frac{dN}{dE_g}(z_g) \frac{dE_g(E, z_g)}{dE}, \quad (23)$$

where $dN/dE_g(z_g)$ is the injection spectrum at redshift z_g and a is a constant depending mainly on the source emissivity. We have calculated $dE_g(E, z_g)/dE$ as it is described in Ref. [51]. For the injection spectrum we have used $dN/dE_g(z_g) \sim E_g^{-2.7}$ with a maximal redshift $z_{\text{max}} = 2$ and both without an intrinsic energy cutoff (Fig. 12) and with a cutoff at $E = 1 \cdot 10^{22}$ eV (Fig. 13).

The calculated diffuse spectra are presented for three different masses of the glueballino, $m_{\tilde{G}} = 1.5, 2$ and 3 GeV, and for comparison the corresponding proton spectra are also shown. The cutoff in the glueballino spectra is shifted to larger energies not only because of $m_{\tilde{G}} > m_N$ but also because of the large mass gap between \tilde{G} and $\tilde{\rho}_{1/2}^*$. Moreover, the smaller cross-section and energy transfer make the cutoff less pronounced. The calculated spectra are for all three masses in agreement with the observations [36]. However, the observed flux above the GZK-cutoff can only be reproduced, if either the glueballino injection spectrum is rather flat or if also at energies $E \sim 10^{19}$ eV glueballinos are a non-negligible component of the cosmic ray flux. Finally, we stress that the exact form of the glueballino energy spectrum depend rather strongly on the mass spectrum of the hadronic bound states of the gluino; still our general observations (shift of the cutoff to larger energies, less pronounced cutoff) are independent of the details of the mass spectrum.

5 Experimental limits from beam-dump experiments

The experiment FNAL-E-0330 by Gustafson *et al.* was designed to search for neutral hadrons with masses $\gtrsim 2$ GeV and lifetimes $\gtrsim 10^{-7}$ s [37]. In contrast to the recent experiments [25, 26, 27, 28], the Gustafson experiment was sensitive to long-lived or stable hadrons. It set upper limits on the production cross-section of these hadrons in the mass range 2–12 GeV which are given in the second line of Table 5. However, the relation between the measured mass, M_{meas} , in the Gustafson experiment and the physical mass of \tilde{g} -hadrons needs careful consideration.

In the Gustafson experiment, short pulses of protons with energy 300 GeV produced in the beam-dump target neutral secondary particles, which were detected in a calorimeter at distance $l = 590$ m from the target. The calorimeter had the total thickness $X_{\text{cal}} = 900$ g/cm², and it was assumed that a particle loses all its energy therein. Then the measured difference in the time of flight δt of massive secondaries and photons determines the mass of the secondary,

$$M_{\text{meas}} = (2cE_{\text{loss}}^2 \delta t/l)^{1/2}. \quad (24)$$

Here, the energy loss E_{loss} in the calorimeter is taken as the energy of a particle. In fact, a \tilde{g} -hadron loses however only a part of its energy in the calorimeter: $E_{\text{loss}}/E = K_{\text{inel}}X_{\text{cal}}/X_{\text{int}}$, where X_{int} is the inelastic interaction length. Then the physical mass $M_{\tilde{G}}$ of a \tilde{g} -hadron is connected with the measured mass as

$$M_{\text{meas}} = (E_{\text{loss}}/E)M_{\tilde{G}}. \quad (25)$$

In the case of a glueballino, one obtains from Eq. (25) together with the data of Table 1 $M_{\text{meas}} \sim 1$ GeV for $M_{\tilde{G}} = 2$ and 5 GeV. Thus, in both cases glueballinos fall in the region of neutron background and therefore these masses are allowed.

Are heavier masses of \tilde{g} -hadrons allowed by the Gustafson experiment?

We have calculated the cross-section for gluino production in pp-collision via the two subprocesses $gg \rightarrow \tilde{g}\tilde{g}$ and $q\bar{q} \rightarrow \tilde{g}\tilde{g}$ at next-to-leading order [52] for $E_{\text{lab}} = 300$ GeV using the program `Prospero` [53]. As parton distributions we have chosen those of Glück,

Reya and Vogt [54], while we have used $Q = m_{\tilde{g}}$ as renormalization and factorization scales. In Table 5, the production cross-sections averaged over the region allowed by the experimental cuts are compared with the upper limits from the Gustafson experiment. The inspection of Table 5 for larger masses shows that the calculated cross-sections are smaller than the upper limits given in the second line. We conclude that the results of the Gustafson experiment do not exclude \tilde{g} -hadrons.

A modified Gustafson experiment has great potential to discover light \tilde{g} -hadrons in the window 2–4 GeV or to reliably exclude it. For this aim, a thicker calorimeter is needed. If \tilde{g} -hadrons lose all their energy in the calorimeter, then $M_{\text{meas}} \approx M_{\tilde{G}}$ and the third and fourth line of Table 5 show that the calculated cross-sections for $M_{\tilde{G}}$ in the interval 2–4 GeV are larger than the experimental upper bounds. It means that \tilde{g} -hadron in this mass window can be discovered or excluded, if the calorimeter is thick enough. Taking into account the large penetrating power of \tilde{g} -hadrons the neutron background can be greatly reduced by placing the absorber behind the target which thickness is tuned to absorb the neutrons but to be transparent for \tilde{g} -hadrons.

The signature of \tilde{g} -hadrons is given by the compatibility of the gluino production cross-section with the measured flux of detected particles. The path-length and the average fraction of lost energy will serve as further indicators. The measured properties of \tilde{g} -hadrons will then allow reliable calculations of \tilde{g} -hadron production in astrophysical sources and their detection in EAS.

6 Conclusions

There are two mass windows where a light gluino is marginally allowed: $m_{\tilde{g}} \lesssim 3$ GeV and $25 \lesssim m_{\tilde{g}} \lesssim 35$ GeV. The first window is disfavoured by the gluino contribution to the running of α_s and to the colour coefficients. The lightest \tilde{g} -hadron is heavier than the gluino by the mass of constituent gluon or quarks. The existence of a light *quasi-stable* \tilde{g} -hadron, corresponding to the first window for gluino masses, crucially depends on whether the neutral or charged \tilde{g} -hadron is the lightest one. A light quasi-stable charged \tilde{g} -hadron is forbidden by the production of “wild hydrogen” in the Earth atmosphere by cosmic rays. The case that the lightest \tilde{g} -hadron is neutral is also forbidden, if it forms a bound state with the proton (“wild deuteron”). The status of the light gluino and lightest \tilde{g} -hadron can further be clarified by further theoretical analysis. At present we conservatively consider the first gluino window as disfavoured, but not excluded.

As the carrier of UHE signal, the light \tilde{g} -hadrons with a mass larger than 1.5 GeV have a spectrum with the GZK cutoff beyond the observed energy range (see Fig. 12). Together with accelerator limits on the gluino mass, $m_{\tilde{g}} < 3$ GeV, it leaves for \tilde{g} -hadron masses the narrow window 1.5–4 GeV. The other window allowed by accelerator experiments is 25–35 GeV.

In this paper we have studied the interaction of \tilde{g} -hadrons with nucleons and nuclei and the development of UHE EAS initiated by such particles. In practice, we have considered the special case of a glueballino as the primary particle. We think, however, that any other \tilde{g} -hadron with equal mass has essentially the same interaction properties.

We have calculated the glueballino-nucleon inelastic and total cross-sections for different masses of glueballinos (see Figs. 1, 2). The longitudinal development of the EAS with energy $3 \cdot 10^{20}$ eV in the atmosphere is shown in Fig. 9. One can see that glueballinos heavier than 5 GeV resemble penetrating particles. The profiles shown in the Figure are directly measured in Fly's Eye experiment, and the data are quite different from the graphs displayed here for heavy glueballinos. The second mass window 25–35 GeV can be already reliably excluded on the basis of these measurements, though a detailed analysis is desirable.

The showers produced by \tilde{g} -hadron from the low-mass window are similar to proton-initiated showers in all characteristics (see the longitudinal profiles in Figs. 3, 5 and 7, the distributions over X_{\max} in Figs. 4, 6 and 8, lateral distributions for electrons and muons in Figs. 10, 11 and fluctuations in muon and electron densities in Tables 3 and 4). In principle, the best possibility to distinguish the showers produced by \tilde{g} -hadron with mass 2 GeV from the proton-induced showers are the fluctuations in the muon density at large distances $d > 600$ m (see Table 3). However, the statistics of the largest array at present, AGASA, is not sufficient for such a discrimination. The large X_{\max} tail in the distribution of showers initiated by \tilde{g} -hadrons over X_{\max} offers for HiRes or AUGER another, more promising possibility to (dis-) prove light gluinos as UHE primaries.

More reliably the quasi-stable 2–3 GeV \tilde{g} -hadron can be found in an especially designed accelerator beam-dump experiment (see section 5). In this experiment, it is possible to discover supersymmetry (light gluino) and to find a new primary for the UHE cosmic signal.

Acknowledgements

We are grateful to Michael Spira for helpful comments about the use of PROSPINO.

References

- [1] G. Auriemma, L. Maiani and S. Petrarca, Phys. Lett. **B164**, 179 (1985).
- [2] V.S. Berezinskii and B.L. Ioffe, Sov. Phys. JETP **63**, 920 (1986) and preprint ITEP, N0 127, 1985.
- [3] D.J. Chung, G.R. Farrar and E.W. Kolb, Phys. Rev. **D57**, 4606 (1998).
- [4] G.R. Farrar and P.L. Biermann, Phys. Rev. Lett. **81**, 3579 (1998).
- [5] For recent reviews see M. Nagano and A.A. Watson, Rev. Mod. Phys. **72**, 689 (2000); P. Bhattacharjee and G. Sigl, Phys. Rep., **327**, 110 (2000); V. Berezinsky, Nucl. Phys. (Proc. Suppl.) **70**, 419 (1999); S. Yoshida and H. Dai, J. Phys. **G24**, 905 (1998).
- [6] K. Greisen, Phys. Rev. Lett. **16**, 748 (1966); G.T. Zatsepin and V.A. Kuzmin, JETP Lett. **4**, 78 (1966).

- [7] N. Hayashida *et al.*, Phys.Rev. Lett. **73** 39, (1994).
- [8] D. Bird *et al.*, Astroph. J. **441**, 144 (1995).
- [9] N. Sakaki (AGASA collaboration), Proc. of 27th Intern. Cosmic Ray Conf. (Hamburg), 333 (2001).
- [10] V. Berezhinsky, M. Kachelrieß and A. Vilenkin, Phys. Rev. Lett. **79**, 4302 (1997); V.A. Kuzmin and V.A. Rubakov, Phys. Atom. Nucl. **61**, 1028 (1998).
- [11] C.T. Hill, D.N. Schramm and T.P. Walker, Phys Rev. **D36**, 1007 (1987).
- [12] T.J. Weiler, Astrop. Phys. **11**, 303 (1999); D. Fargion, B. Mele and A. Salis, Ap. J. **517**, 725 (1999); G. Gelmini and A. Kusenko, Phys. Rev. Lett. **82**, 5202 (1999) and **84**, 1378 (2000).
- [13] V.S. Berezhinsky and G.T. Zatsepin, Phys. Lett. **B28**, 423 (1969); G. Domokos and S. Nussinov, Phys. Lett. **B187**, 372 (1987); J. Bordes, H. Chan, J. Faridani, J. Pfaudler and S.T. Tsou, Astropart. Phys. **8**, 135 (1998); G. Domokos and S. Kovesi-Domokos, Phys. Rev. Lett. **82**, 1366 (1999); P. Jain, D.W. McKay, S. Panda and J.P. Ralston, Phys. Lett. B **484**, 267 (2000); but see also G. Burdman, F. Halzen and R. Gandhi, Phys. Lett. B **417**, 107 (1998); M. Kachelrieß and M. Plümacher, Phys. Rev. D **62**, 103006 (2000).
- [14] T.W. Kephart and T.J. Weiler, Astrop.Phys. **4**, 271 (1996); S. Bonazzola and P. Peter, Astrop. Phys. **7**, 161 (1997).
- [15] L. Gonzales-Mestres, Nucl. Phys. B (Proc.Suppl.) **48**, 131 (1996); S. Coleman and S.L. Glashow, Phys. Rev. **D 59**, 116008 (1999); R. Aloisio, P. Blasi, P. Ghia, and A. Grillo, Phys. Rev. D **62**, 053010 (2000)
- [16] G. Sigl, D.F. Torres, L.A. Anchordoqui and G.E. Romero, Phys. Rev. D **63**, 081302 (2001); A. Virmani, S. Bhattacharya, P. Jain, S. Razzaque, J.P. Ralston and D.W. McKay, astro-ph/0010235; P.G. Tinyakov and I.I. Tkachev, astro-ph/0102476; L.A. Anchordoqui *et al.*, astro-ph/0106501.
- [17] V. Berezhinsky and M. Kachelrieß, Phys. Lett. **B422**, 163 (1998).
- [18] F. Halzen, R.A. Vazquez, T. Stanev and H.P. Vankov, Astrop.Phys. **3**, 151 (1995).
- [19] N.N. Kalmykov, S.S. Ostapchenko and A.I. Pavlov, Phys. At. Nucl. **58**, N10, 1728 (1995).
- [20] G.R. Farrar, Phys. Rev. Lett. **76**, 4111 (1996).
- [21] S. Raby, Phys. Lett. **B422**, 158 (1998).
- [22] S. Raby and K. Tobe, Nucl. Phys. **B539**, 3 (1999).

- [23] M.B.Voloshin and L.B.Okun, Sov.J.Nucl.Phys. **43**, 495 (1986).
- [24] F.Buccella, G.R.Farrar, and A.Pugliese, Phys.Lett. **B 153**, 311 (1985).
- [25] J. Adams *et al.* [KTeV Collaboration], Phys. Rev. Lett. **79**, 4083 (1997)
- [26] V. Fanti *et al.* [NA48 Collaboration], Phys. Lett. **B446**, 117 (1999).
- [27] A. Alavi-Harati *et al.* [KTeV Collaboration], Phys. Rev. Lett. **83**, 2128 (1999).
- [28] I.F. Albuquerque *et al.* [E761 Collaboration], Phys. Rev. Lett. **78**, 3252 (1997).
- [29] F. Csikor and Z. Fodor, Phys. Rev. Lett. **78**, 4335 (1997).
- [30] R. Barate *et al.* [ALEPH Collaboration], Z. Phys. **C76**, 1 (1997).
- [31] G.R. Farrar, Nucl. Phys. Proc. Suppl. **62**, 485 (1998).
- [32] C. Caso *et al.* (Particle Data Group), Eur. J. Phys. **C3**, 1 (1998).
- [33] H. Baer, K. Cheung, J.F. Gunion, Phys. Rev. **D59**, 075002 (1999).
- [34] A. Mafi and S. Raby, Phys. Rev. D **62**, 035003 (2000).
- [35] R.N. Mohapatra and S. Nussinov, Phys. Rev. **D57**, 1940 (1998).
- [36] M. Takeda *et al.*, Phys. Rev. Lett. **81**, 1163 (1998).
- [37] H.R. Gustafson *et al.*, Phys. Rev. Lett. **37**, 474 (1976).
- [38] I.F. Albuquerque, G.R. Farrar and E.W. Kolb, Phys. Rev. **D59**, 015021 (1999).
- [39] N.N. Kalmykov, S.S. Ostapchenko and A.I. Pavlov, Nucl. Phys. (Proc. Suppl.) **52B**, 17 (1997); N.N. Kalmykov and S.S. Ostapchenko, Preprint INP MSU 98-36/537, Moscow 1998.
- [40] N.N. Kalmykov, S.S. Ostapchenko and A.I. Pavlov, Izv. RAN Ser. Fiz. **58**, 21 (1994) (English translation in Bull.Russ.Acad.Sci (USA), Phys.Ser. **v.58** 1966 (1994).)
- [41] J.Hoerandel, Proc. of the 26th ICRC, Salt Lake City, **v.1** 131 (1999).
- [42] A.B. Kaidalov and K.A. Ter-Martirosyan, Phys. Lett. **B117** 247 (1982).
- [43] R.J. Glauber in "Lectures in theoretical physics", Amsterdam, 1967.
- [44] V.N. Gribov, ZhETF **59**, 892 (1969) (in Russian).
- [45] N.N. Kalmykov and S.S. Ostapchenko, Phys. At. Nucl. **56**, 346 (1993).
- [46] S. Ostapchenko, T. Thouw and K. Werner, Nucl. Phys. (Proc. Suppl.) **52B**, 3 (1997).
- [47] G. Marchesini and B.R. Webber, Nucl.Phys. **B238**, 1 (1984).

- [48] D.J. Bird *et al.*, *Astroph. J.* **441**, 144 (1995).
- [49] M. Chanowitz and S. Sharpe, *Phys. Lett.* **B126**, 227 (1983). We use the vales given in their table 2 for $C_{TE} = 1$.
- [50] V.S. Berezinsky, S.V. Bulanov, V.L. Ginzburg, V.A. Dogiel and V.S. Ptuskin, *Astrophysics of Cosmic Rays*, chapter 4, Elsevier 1990.
- [51] V.S. Berezinsky and S.I. Grigorieva, *Astron. Astrophys.* **199**, 1 (1988).
- [52] W. Beenakker, R. Höpker, M. Spira and P.M. Zerwas, *Nucl. Phys. B* **492**, 51 (1997)
- [53] W. Beenakker, R. Höpker and M. Spira, hep-ph/9611232.
- [54] M. Glück, E. Reya and A. Vogt, *Z. Phys.* **C67**, 433 (1995).

	π	$M_{\tilde{G}} = 2 \text{ GeV}$	$M_{\tilde{G}} = 5 \text{ GeV}$	$M_{\tilde{G}} = 10 \text{ GeV}$	$M_{\tilde{G}} = 50 \text{ GeV}$
σ_{tot}	24.4	3.9	2.9	2.4	2.2
σ_{in}	20.9	3.8	2.8	2.4	2.1
$\sigma_{\text{tot}}^{\text{s-coupl}}$		3.8	2.7	2.4	2.2
$\sigma_{\text{tot}}^{\text{d-coupl}}$		0.14	0.15	0.013	0
σ_{AFK}		3.8	2.7	2.4	2.2
K_{inel}		0.25	0.15	0.074	0.0054

Table 1: Total cross-section σ_{tot} , inelastic cross-section σ_{in} , cross-section due to soft coupling $\sigma_{\text{tot}}^{\text{s-coupl}}$, cross-section due to direct coupling $\sigma_{\text{tot}}^{\text{d-coupl}}$, cross-section without hard interactions σ_{AFK} and the inelasticity coefficient K_{inel} for the glueballino-nucleon scattering. The data are given for four values of the glueballino mass $M_{\tilde{G}}$ from 2 GeV to 50 GeV at glueballino energy $E_{\text{lab}} = 100 \text{ GeV}$. As references, the total and inelastic cross-section of the pion are also given. All cross-sections are in mbarn.

	π	$M_{\tilde{G}} = 2 \text{ GeV}$	$M_{\tilde{G}} = 5 \text{ GeV}$	$M_{\tilde{G}} = 10 \text{ GeV}$	$M_{\tilde{G}} = 50 \text{ GeV}$
σ_{tot}	152	103	94.9	91.3	88.0
σ_{in}	112	71.3	65.9	63.4	60.2
$\sigma_{\text{tot}}^{\text{s-coupl}}$		85.5	69.4	61.8	50.8
$\sigma_{\text{tot}}^{\text{d-coupl}}$		72.1	72.4	72.3	74.4
σ_{AKF}	92.2	18.2	13.3	11.8	10.6
K_{inel}		0.26	0.14	0.082	0.018

Table 2: The same as Table 1 for $E_{\text{lab}} = 10^{12} \text{ GeV}$.

R, m	10	50	100	200	300 m	600 m	1200 m
proton	0.077	0.054	0.068	0.095	0.11	0.15	0.18
$\tilde{G}(2 \text{ GeV})$	0.20	0.25	0.27	0.30	0.31	0.34	0.36
$\tilde{G}(5 \text{ GeV})$	0.33	0.37	0.39	0.41	0.43	0.45	0.47
$\tilde{G}(10 \text{ GeV})$	0.40	0.43	0.45	0.47	0.48	0.50	0.52

Table 3: Normalized 1σ fluctuations of the electron LDF $\sigma_{\rho_e(R)}/\rho_e(R)$ at the AKENO observation level for EAS of energy $E_0 = 10^{20} \text{ eV}$ initiated by protons and glueballinos of masses 2, 5 and 10 GeV.

R, m	10	100	200	300 m	600 m	1200 m
proton	0.19	0.16	0.16	0.17	0.20	0.25
$\tilde{G}(2 \text{ GeV})$	0.18	0.20	0.24	0.27	0.33	0.41
$\tilde{G}(5 \text{ GeV})$	0.23	0.30	0.34	0.37	0.43	0.51
$\tilde{G}(10 \text{ GeV})$	0.30	0.36	0.40	0.42	0.48	0.55

Table 4: Normalized 1σ fluctuations of the muon LDF ($E_\mu > 1 \text{ GeV}$) $\sigma_{\rho_\mu(R)}/\rho_\mu(R)$ at the AKENO observation level for EAS of energy $E_0 = 10^{20} \text{ eV}$ initiated by protons and glueballinos of masses 2, 5 and 10 GeV.

$M_{\text{meas}}/\text{GeV}$	2	3	4	6	8	10
90% C.L.	1.0e-32	3.6e-33	1.3e-33	5.3e-33	2.0e-33	1.7e-33
$m_{\tilde{g}}/\text{GeV}$	2	3	4	6	8	10
$E d^3\sigma/d^3p$	3.8e-30	1.7e-31	1.1e-32	4.2e-35	3.9e-38	8.9e-43

Table 5: The upper 90% C.L. limit on the invariant cross-sections $E d^3\sigma/d^3p$ (second line) for measured masses M_{meas} (first line) given by the Gustafson experiment. The fourth line gives the calculated invariant cross-sections for gluino production in pp-interaction at $E_{\text{p,lab}} = 300 \text{ GeV}$ and for gluino mass $m_{\tilde{g}}$ (third line). All cross-sections are in cm^2/GeV^2 .

$m_{\tilde{g}}/\text{GeV}$	0.64	1.04	1.48	2.41
$M_{\tilde{G}}/\text{GeV}$	1.00	1.50	2.00	3.00
$m_{\tilde{\rho}_{1/2}}/\text{GeV}$	1.17	1.58	2.04	3.03

Table 6: The masses of the glueballino \tilde{G} and the $\tilde{\rho}_{1/2}$ as function of the gluino mass $m_{\tilde{g}}$ according to Ref. [49].

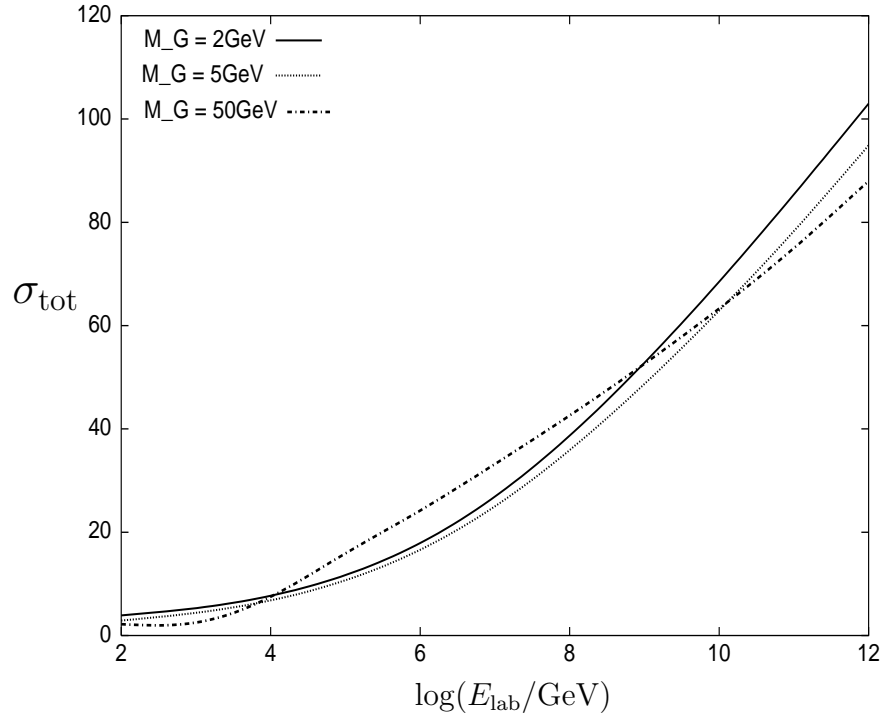


Figure 1: Total glueballino-nucleon cross-section σ_{tot} in mbarn as function of E_{lab} for $M_{\tilde{G}} = 2, 5$ and 50 GeV.

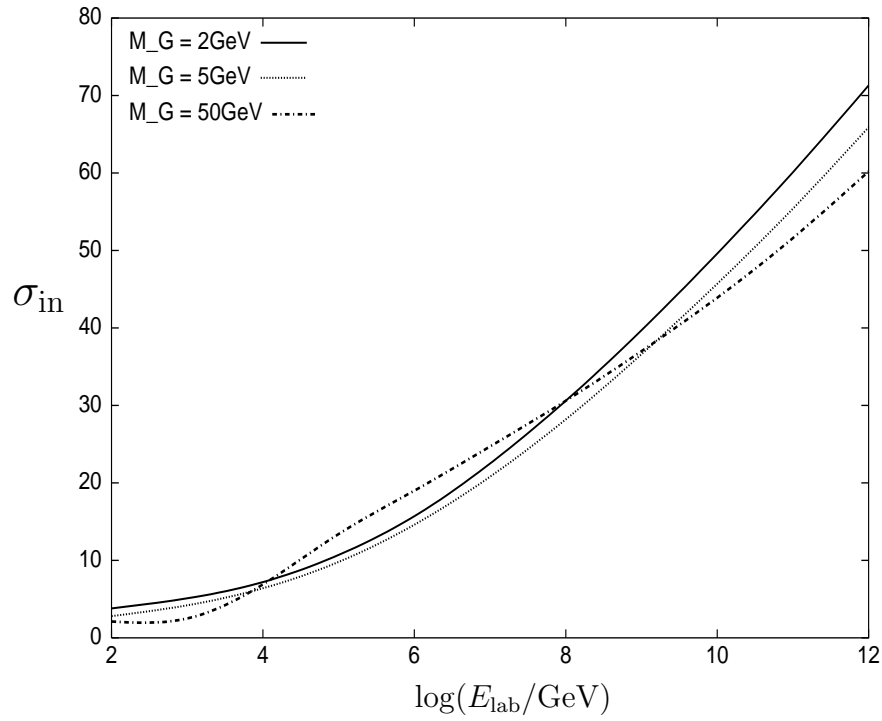


Figure 2: Inelastic glueballino-nucleon cross-section σ_{in} in mbarn as function of E_{lab} for $M_{\tilde{G}} = 2, 5$ and 50 GeV.

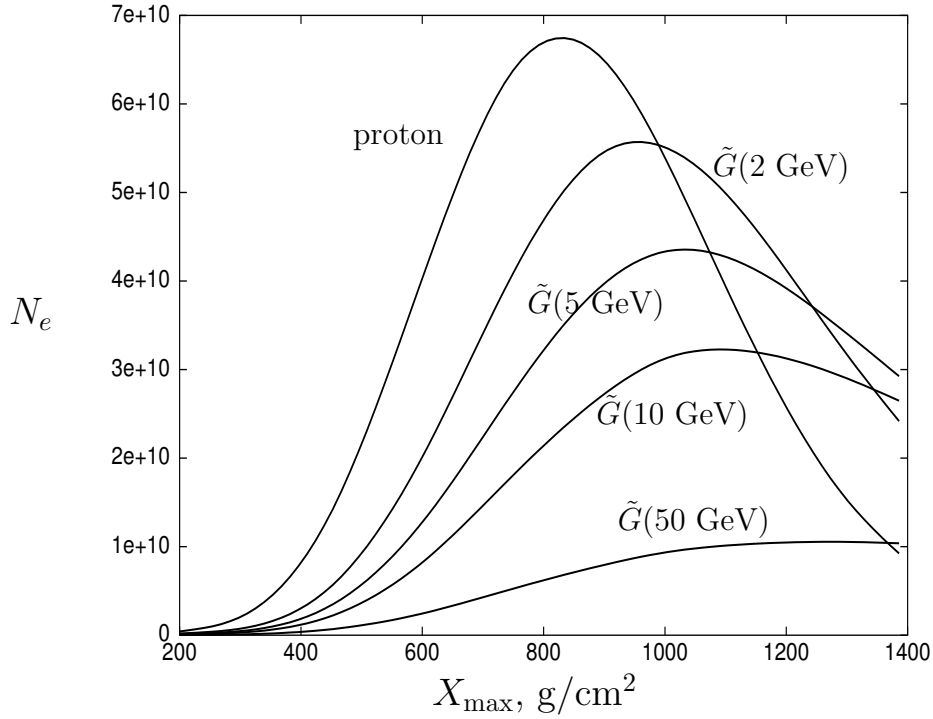


Figure 3: Longitudinal shower profile for EAS of energy $E_0 = 10^{20}$ eV initiated by protons and by glueballinos with $M_{\tilde{g}} = 2, 5, 10$ and 50 GeV.

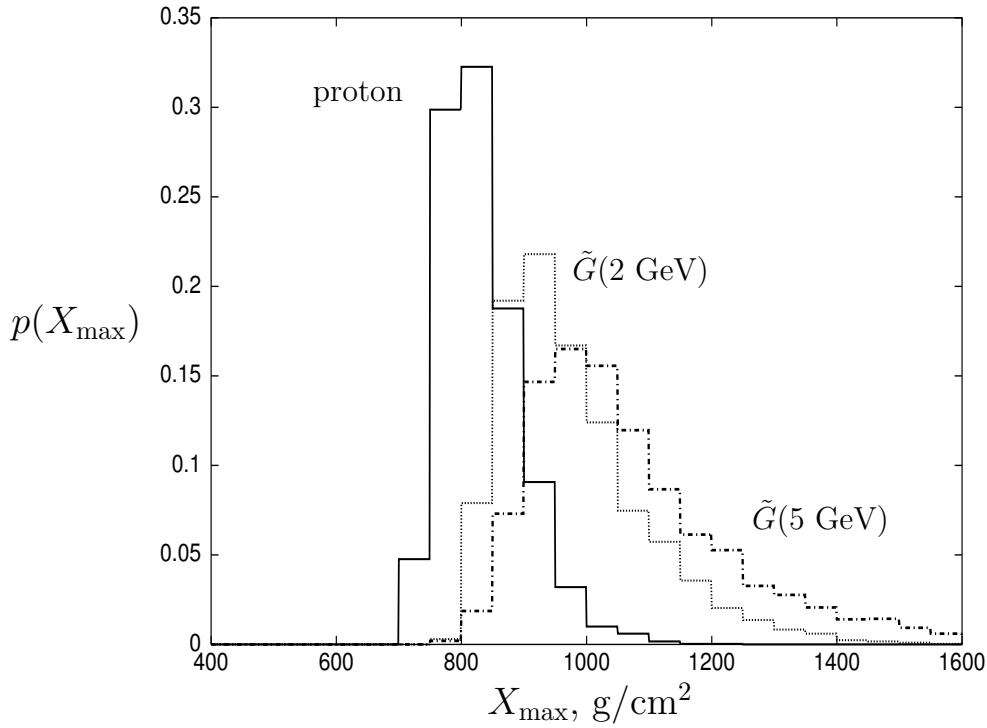


Figure 4: Normalized distribution $p(X_{\max})$ of the shower maxima for EAS of energy $E_0 = 10^{20}$ eV initiated by protons and by glueballinos with $M_{\tilde{g}} = 2$ and 5 GeV.

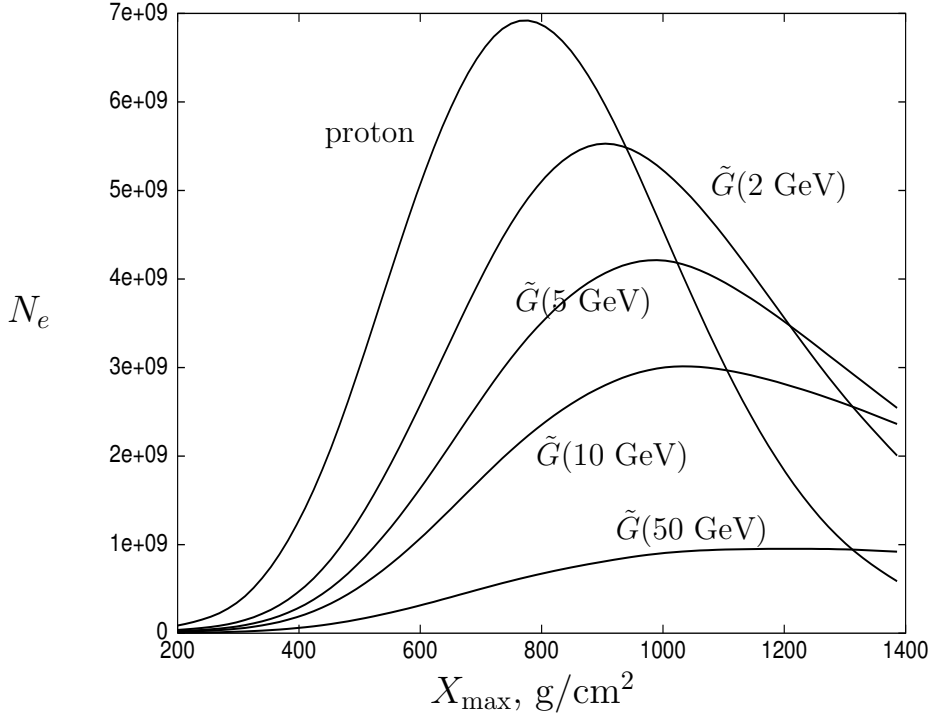


Figure 5: Longitudinal shower profile for EAS of energy $E_0 = 10^{19}$ eV initiated by protons and by glueballinos with $M_{\tilde{g}} = 2, 5, 10$ and 50 GeV.

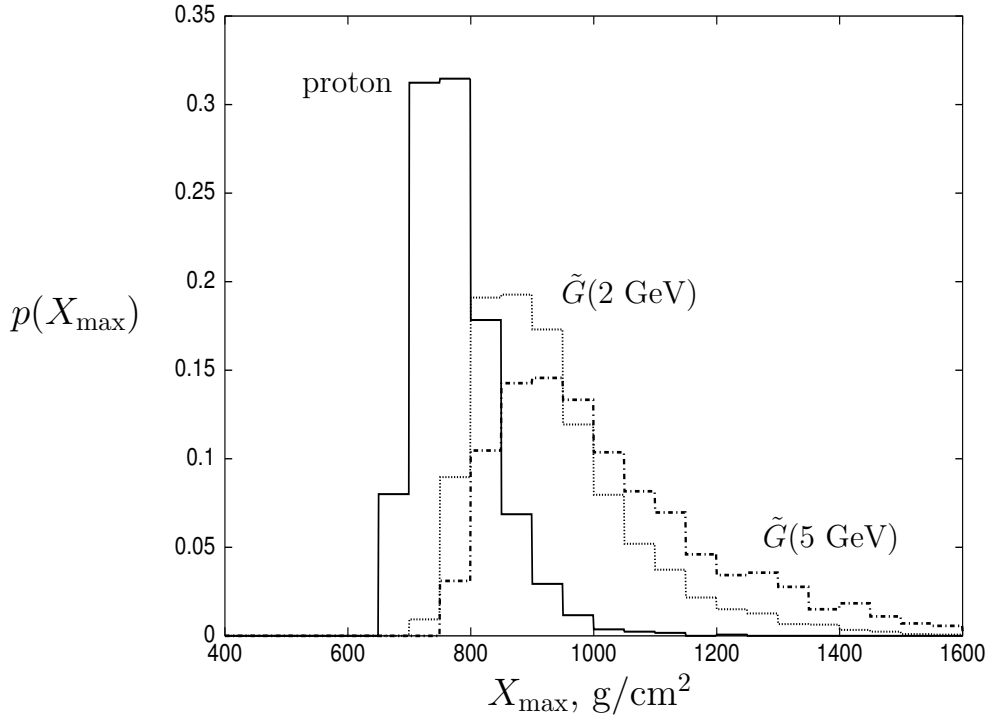


Figure 6: Normalized distribution $p(X_{\max})$ of the shower maxima for EAS of energy $E_0 = 10^{19}$ eV initiated by protons and by glueballinos with $M_{\tilde{g}} = 2$ and 5 GeV.

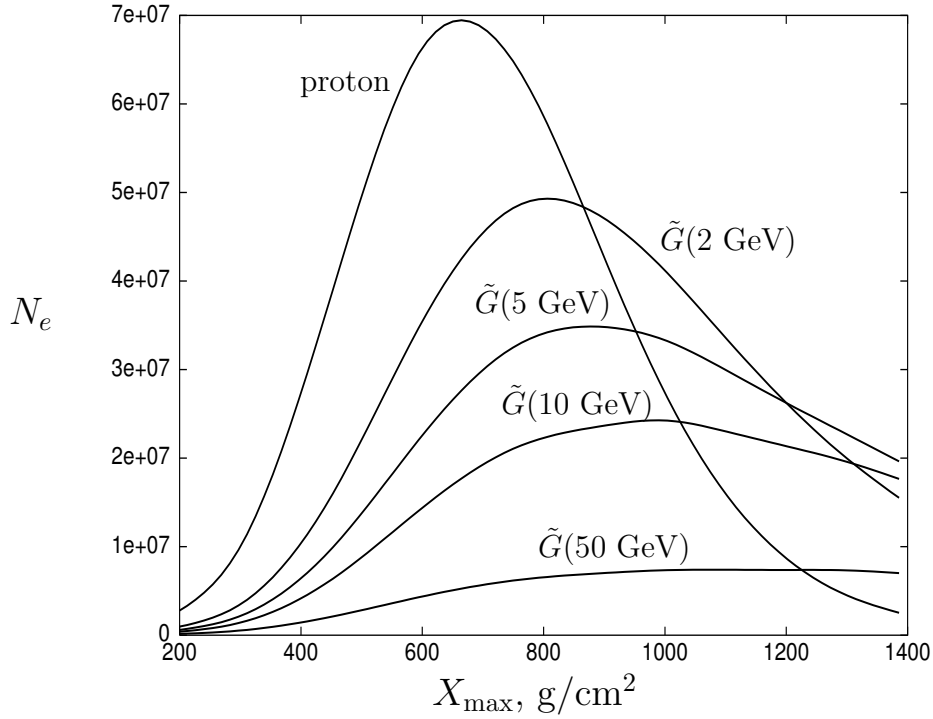


Figure 7: Longitudinal shower profile for EAS of energy $E_0 = 10^{17}$ eV initiated by protons and by glueballinos with $M_{\tilde{g}} = 2, 5, 10$ and 50 GeV.

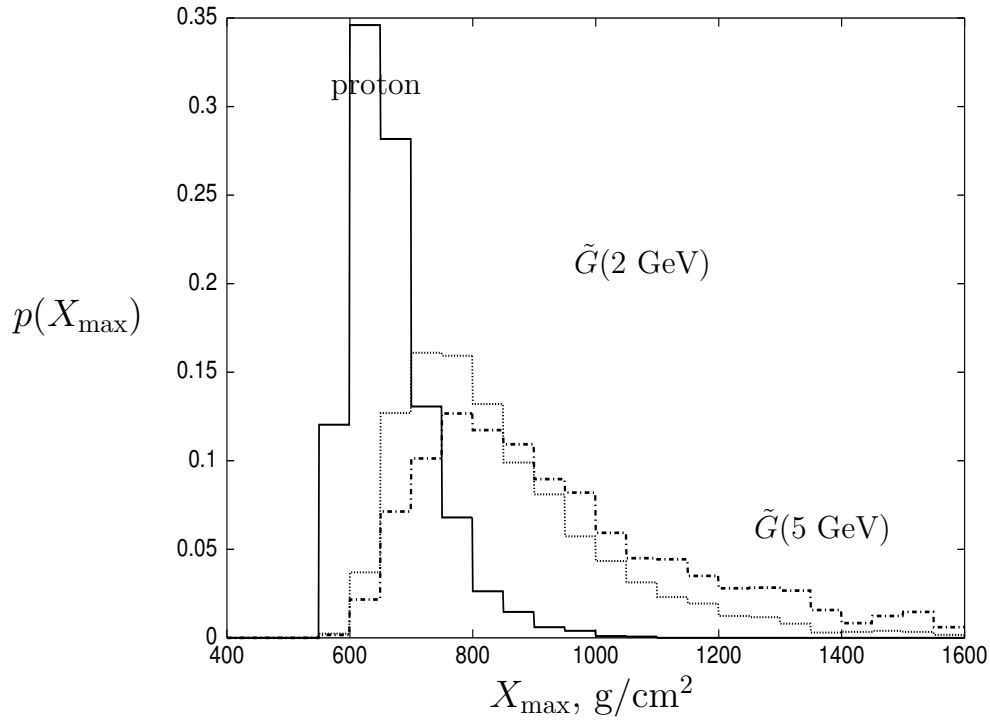


Figure 8: Normalized distribution $p(X_{\max})$ of the shower maxima for EAS of energy $E_0 = 10^{17}$ eV initiated by protons and by glueballinos with $M_{\tilde{g}} = 2$ and 5 GeV.

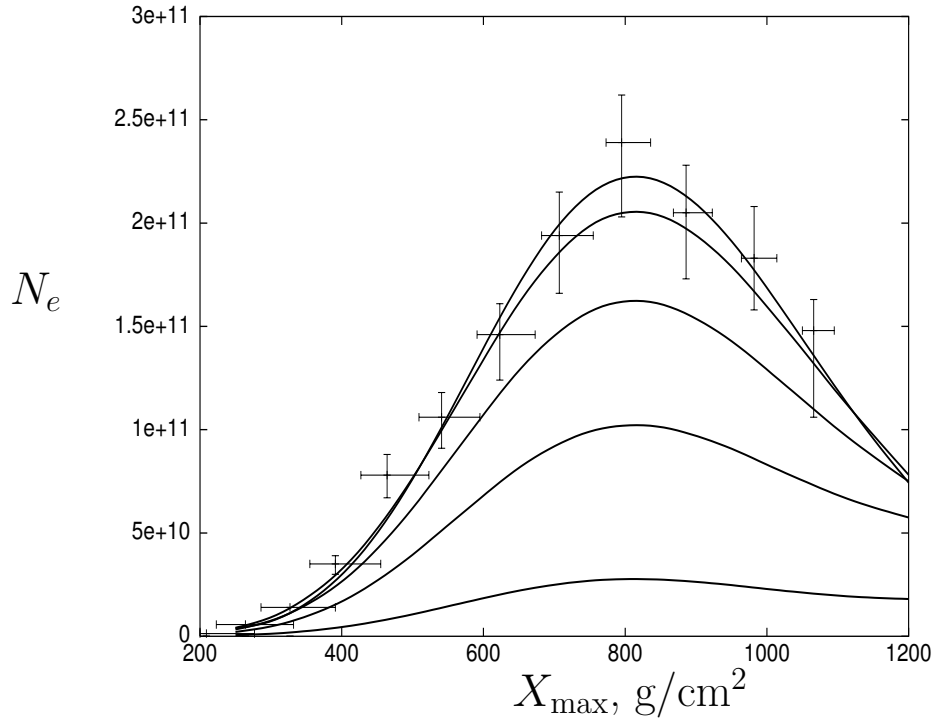


Figure 9: Comparison of Flye’s Eye highest energy event with the longitudinal shower profile for EAS of energy $E_0 = 3 \times 10^{20}$ eV initiated (from top to down) by protons and by glueballinos with $M_g = 2, 5, 10$ and 50 GeV. The shower profiles are shifted so that their X_{max} agrees with the observed shower maximum.

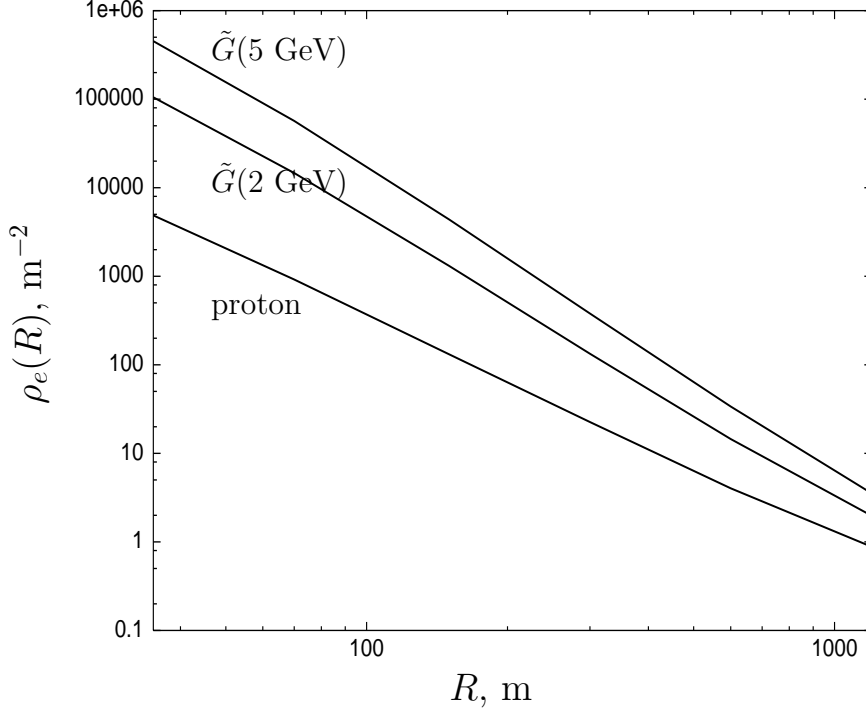


Figure 10: Electron *LDF* $\rho_e(R)$ in m^{-2} at the AKENO observation level as function of the distance R (in m) from the shower core for EAS of energy $E_0 = 10^{20}$ eV initiated by protons and by glueballinos with $M_{\tilde{g}} = 2$ and 5 GeV.

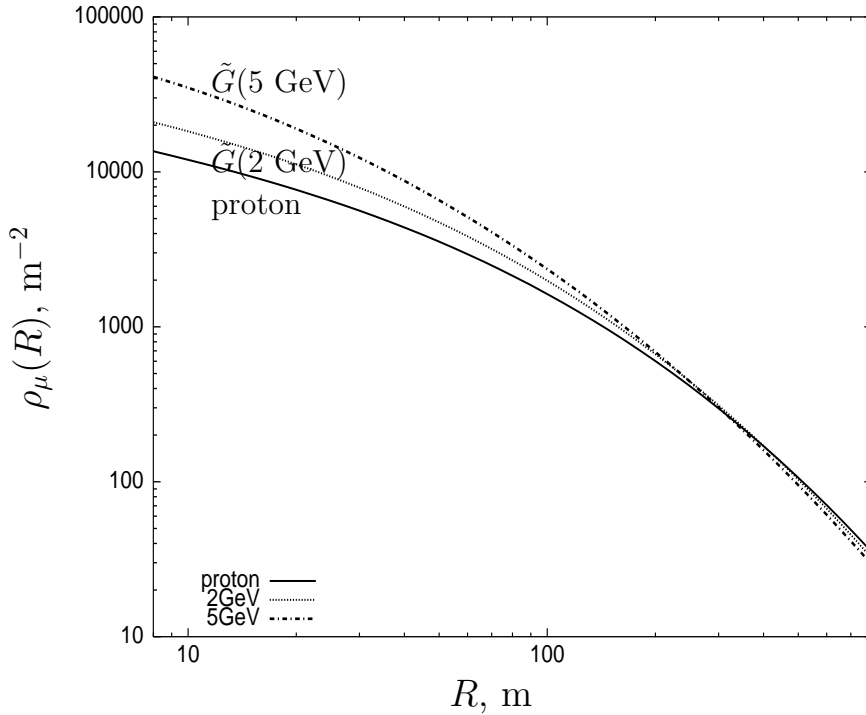


Figure 11: Muon *LDF* ($E_\mu > 1$ GeV) $\rho_\mu(R)$ in m^{-2} at the AKENO observation level as function of the distance R (in m) from the shower core for EAS of energy $E_0 = 10^{20}$ eV initiated by protons and by glueballinos with $M_{\tilde{g}} = 2$ and 5 GeV.

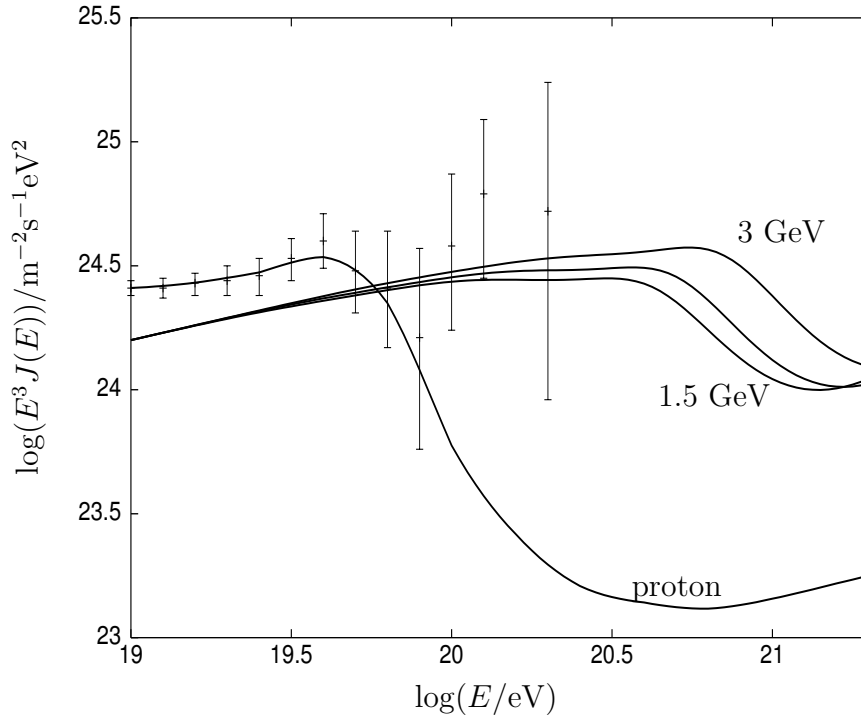


Figure 12: Diffuse glueballino flux from uniformly distributed sources with injection spectra $dN/dE \propto E^{-2.7}$ for $M_{\tilde{G}} = 1.5, 2,$ and 3 GeV, compared with proton flux and observational data from AGASA. Either the gluino flux or a combination of proton and gluino fluxes can fit the data.

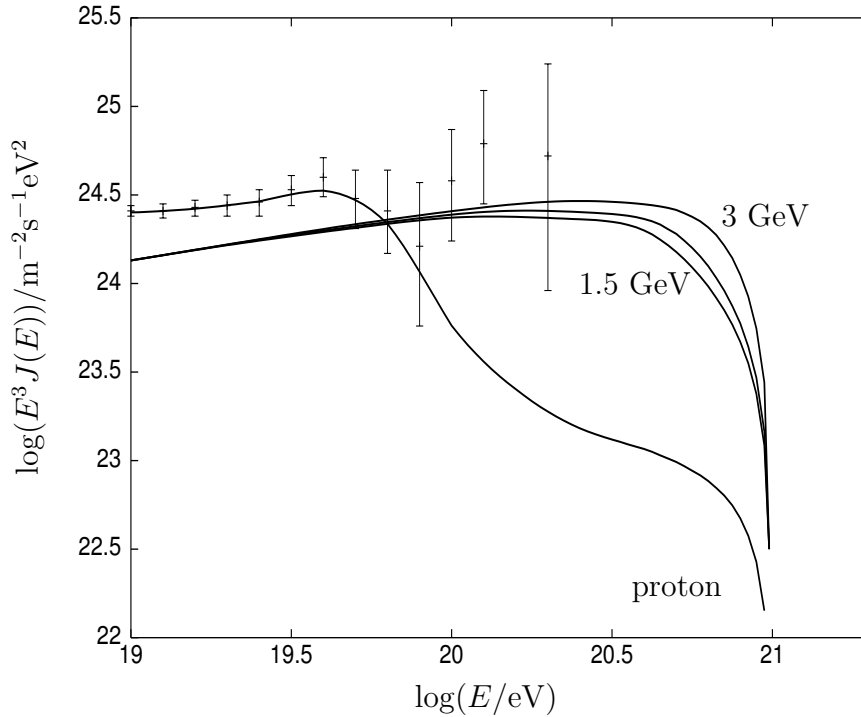


Figure 13: Diffuse glueballino flux from uniformly distributed sources with injection spectra $dN/dE \propto E^{-2.7}$ and intrinsic cutoff $E = 10^{21}$ eV for $M_{\tilde{G}} = 1.5, 2,$ and 3 GeV, compared with proton flux and observational data from AGASA. Either the gluino flux or a combination of proton and gluino fluxes can fit the data.